ACTA IMEKO
ISSN: 2221-870X
September 2025, Volume 14, Number 3, 1 - 5

Evaluating Tip-Enhanced Raman Spectroscopy as a metrological tool for the determination of the number of graphene layers at the nanoscale

Juan D. Caicedo[1,2,3], Tales F. S. Dias[2], Braulio S. Archanjo[2], Thiago L. Vasconcelos[2]

[1] *Postgraduate Metrology Programme, National Institute of Metrology, Quality, and Technology, Duque de Caxias, Rio de Janeiro 25250–020, Brazil*
[2] *Materials Metrology Division, National Institute of Metrology, Quality, and Technology, Duque de Caxias, Rio de Janeiro 25250−020, Brazil*
[3] *Nuclear Technology Development Center – CDTN, Belo Horizonte, Minas Gerais 31270-901, Brazil*

ABSTRACT
This paper presents a comparative analysis of adjacent single and bilayer graphene samples using micro-Raman spectroscopy and Tip-Enhanced Raman Spectroscopy (TERS) techniques. The measurements were carried out close to the diffraction limit, enabling a highly accurate characterization of the graphene layers by TERS and micro-Raman spectroscopy. Hence, TERS experiments yield significantly improved reliability, ensuring more accurate results, since it reduced the region where the number of layers was unknown from around 500 nm for micro-Raman spectroscopy, with a 1.4 numerical aperture objective, to around 60 nm for TERS.

Section: RESEARCH PAPER

Keywords: Tip-Enhanced Raman Spectroscopy; graphene; single-layer graphene; bilayer graphene; metrology

Citation: J. D. Caicedo, T. F. S. Dias, B. S. Archanjo, T. L. Vasconcelos, Evaluating Tip-Enhanced Raman Spectroscopy as a metrological tool for the determination of the number of graphene layers at the nanoscale, Acta IMEKO, vol. 14 (2025) no. 3, pp. 1-5. DOI: 10.21014/actaimeko.v14i3.1948

Section Editor: Daniel Ramos Louzada, PósMQI/PUC-Rio, Rio de Janeiro, Brazil

Received October 18, 2024; **In final form** September 21, 2025; **Published** September 2025

Funding: This work was supported by Coordenação de Aperfeiçoamento de Pessoal de Nível Superior (CAPES) and the Conselho Nacional de Desenvolvimento Científico e Tecnológico (CNPq).

Corresponding author: Thiago L. Vasconcelos, e-mail: tlvasconcelos@inmetro.gov.br

1. INTRODUCTION

Graphene is a 2D material that has been widely studied due to its unique properties and several applications [1]–[7]. Therefore, the ISO Technical Committee 229 and IEC Technical Committee 113 released the ISO/TS 21356-1:2021 standard to help the adaptation of graphene in the industry, which holds the potential to significantly enhance next-generation technology [8]. This standard focuses on several essential properties, including lateral size and the number of layers. To accurately measure these properties, the recommended methods are scanning electron microscopy, atomic force microscopy, and Raman analysis. In this context, Graf et al. [9] used micro-Raman to map an area with adjacent Single-Layer Graphene (SLG) and Bilayer Graphene (BLG) sections, comparing the intensities and positions of the G and 2D bands. Schmidt et al. [10] used the combination of micro-Raman microscopy with Atomic Force Microscopy (AFM), independently, to analyse the height of graphene, the intensities, and the positions of the G and 2D bands. However, conventional Raman spectroscopy (micro-Raman) poses a limitation, requiring flakes larger than the probe size of the instrument (typically from 500 nm to 1 μm) [11]. This limitation can be solved with the use of TERS, which combines the optical microscopy system with a scanning probe microscopy system to be capable of imaging, studying, and broadly characterizing 2D materials on scales far beyond the diffraction limit (similar in dimensions to the probe apex < 30 nm) [12]–[15]. Despite these advantages, TERS experiments have not yet been incorporated into the ISO/TS 21356-1:2021 standard.

An area where the utilisation of TERS can offer advantages is in the clusterisation of the number of graphene layers at the nanoscale. Rabelo et al. [16] employed TERS to examine defects in graphene nanoflakes, correlating the findings with micro-Raman measurements.

Here, we applied TERS on the analyses of an SLG to BLG transition at the nanoscale. The ratio between the intensities of the graphene 2D and G bands, as well as their spectral positions, was used to determine whether the sample is SLG or BLG in the so-called region of indetermination, where micro-Raman cannot differentiate them. Additionally, we present a hyperspectral image, generated from the intensity of the graphene's G band and 2D band, in an area smaller than the micro-Raman spot.

2. MATERIALS AND METHODS

Graphene was mechanically exfoliated from natural graphite and subsequently deposited onto thin glass coverslips. The confocal micro-Raman images were acquired using a Nikon inverted microscope equipped with a 60x oil immersion objective (numerical aperture: 1.4), complemented by a helium–neon laser ($\lambda = 632.8\ nm$). Specifically, we conducted imaging for the 2D and G bands, employing Avalanche Photodiode (APD) detection. For the 2D band, we utilized a bandpass filter centred at 760 nm with a full-width half-maximum (FWHM) of 10 nm. Similarly, for the G band, we employed a slightly tilted bandpass filter centred at 710 nm with a FWHM of 10 nm. The images were acquired at a size of 10 µm x 10 µm (256 pixels x 256 pixels) with a rapid acquisition time of 10 ms. For spectral acquisition, as well as for the hyperspectral line profile, an Andor Shamrock model 303i-A equipped with a Blaze (600 lines/mm grating) was employed. The relative Raman intensity of the spectrometer was calibrated using a stable tungsten halogen light source.

The nano-Raman measurements in this study were conducted using a home-built TERS system (the configuration has been previously described in detail in [12]). A Plasmon-Tunable Tip Pyramid (PTTP) with an apex radius of approximately 30 nm and a nanopyramid base size of $L = 475$ nm was used in order to enhance the local electromagnetic field. The Localized Surface Plasmon Resonance (LSPR) at the tip apex was adjusted to match the red laser excitation wavelength, resulting in strong spectral enhancement within the Near-Field (NF) region [15], [17].

Subsequently, a TERS and a micro-Raman hyperspectral line-profile with a length of 900 nm was performed across the SLG and BLG interface. The pixel distances were set to 37.5 nm and the integration time to 30 s for both Far-Field (FF) and NF measurements. To ensure robustness and obtain reliable data, the acquisition process was repeated four times.

Finally, utilising the TERS, we performed hyperspectral mapping over an area of 640 nm × 320 nm. A total of 2,048 spectra were acquired during this mapping, with an integration time of 1 s.

3. RESULTS AND DISCUSSION

This section describes the measurements performed on areas with adjacent SLG and BLG, as characterised above. Figure 1a shows an APD image obtained using a 2D bandpass filter. Notably, the graphene regions (highlighted by more intense areas) and the glass substrate (darker regions) are distinctly discernible. Figure 1b depicts an APD image acquired using a G bandpass filter. In addition to distinguishing between graphene and glass, it is also possible to differentiate BLG (more intense areas) from single-layer graphene (less intense areas). The Raman spectrum of SLG (gray) and BLG (blue) is presented in Figure 1c. The distinction between the two can be confirmed by using the I_{2D}/I_G criteria, with values of 3.2 indicating an SLG and 0.98 indicating a BLG for the incident laser wavelength used.

Figure 2 presents an analysis of the spectra obtained from the hyperspectral profile acquired along the black dashed line shown in Figure 1b, for the micro-Raman (at left) and TERS (at right). Figure 2a and Figure 2b show the 2D (black) and G (blue) bands' intensities. In Figure 2b, a notable variation in the intensity of the G and 2D bands is observable, indicating a characteristic behaviour associated with a transition from SLG to BLG in the range of 60 nm, limited by the optical resolution of TERS in this experiment. On the contrary, Figure 2a exhibits a more gradual change, which poses a challenge in distinguishing between an SLG and a BLG. This discrepancy is attributed to the spatial resolution of TERS and micro-Raman [18], [19]. Figure 2c and 2d exhibit the variation of the 2D (black) and G (blue) bands' peak spectral position. In Figure 2d, once again, a noticeable shift in the 2D peak position is observed, indicating a transition from an SLG to a BLG, as was observed in Figure 2b. The same is not observed for the G band, which remains almost constant through the transition from single to bilayer graphene at micro and nano-Raman. Figure 2f displays the variation in the full width at half maximum (FWHM) of the 2D band. The observed variation, ranging from ~28 cm^{-1} to ~47 cm^{-1}, can be attributed to the transition from SLG to BLG. This deduction finds confirmation in the fact that graphene with additional layers demonstrates a FWHM greater than 60 cm^{-1} [20]. The image clearly demonstrates a significant variation behaviour associated with the transition from a single layer to bilayer. On the other hand, Figure 2e illustrates a more gradual change in the FWHM of the 2D band, posing a challenge when attempting to differentiate between an SLG and a BLG structure. In all of them, the micro-Raman results remain unclear in the range between 200 nm and 780 nm, the so-called inconclusive region for FF experiments.

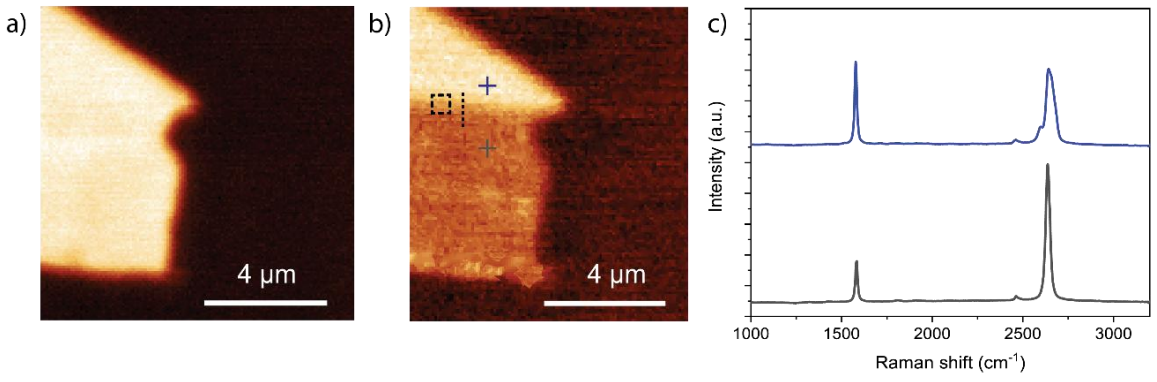

Figure 1. APD images of a graphene sample. The colour scale represents the intensity of the different features: a) 2D band, b) G band, c) Raman spectra of SLG and BLG associated with the graphene sample.

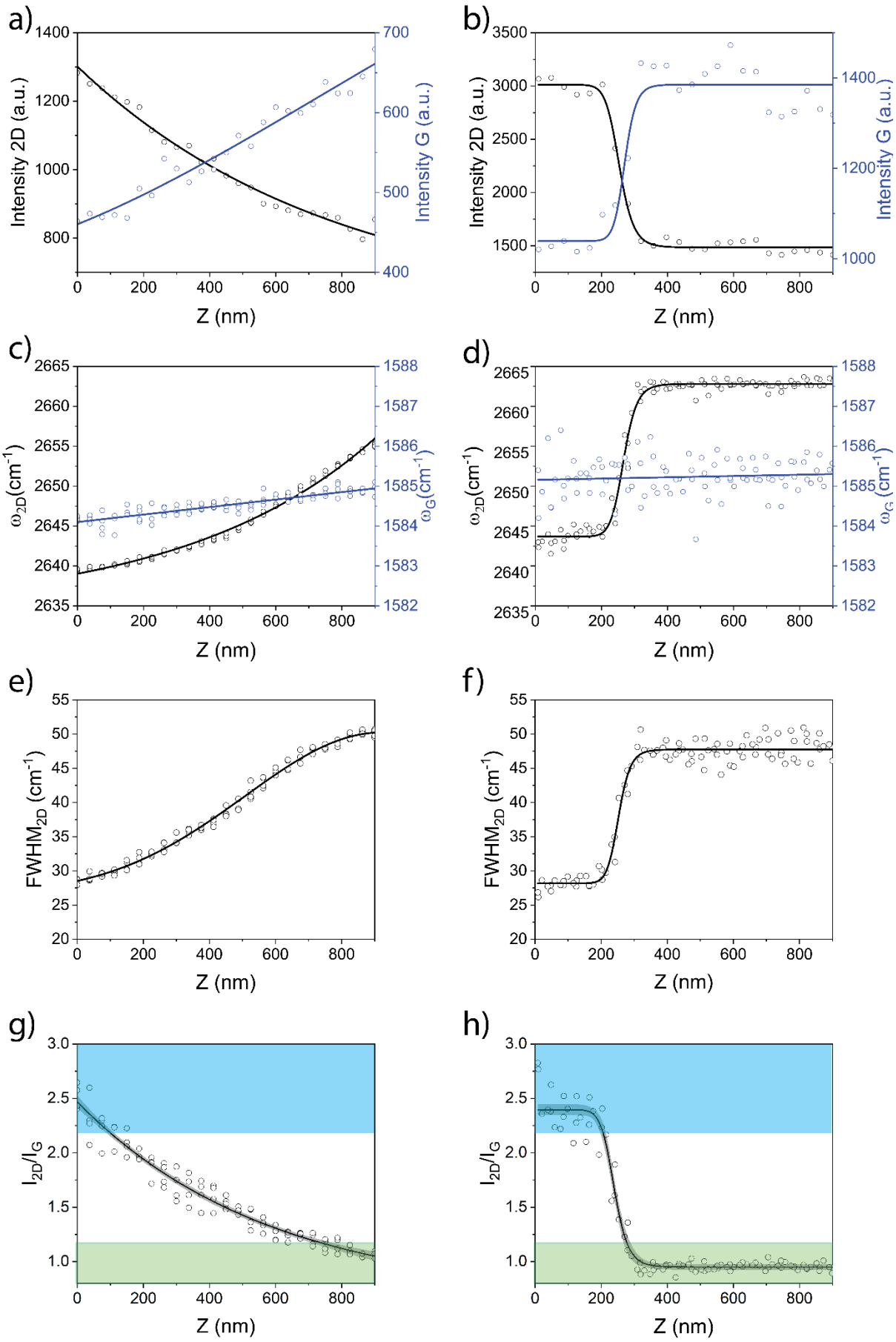

Figure 2. The first and second columns show images generated from the micro-Raman and TERS hyperspectral profile, along the black dashed line in Figure 1b; a) and b) intensities of the 2D band (black) and G band (blue); c) and d) spectral positions of the 2D band (black) and G band (blue); e) and f) full width at half maximum (FWHM) for the 2D band; g) and h) the I_{2D}/I_G ratio.

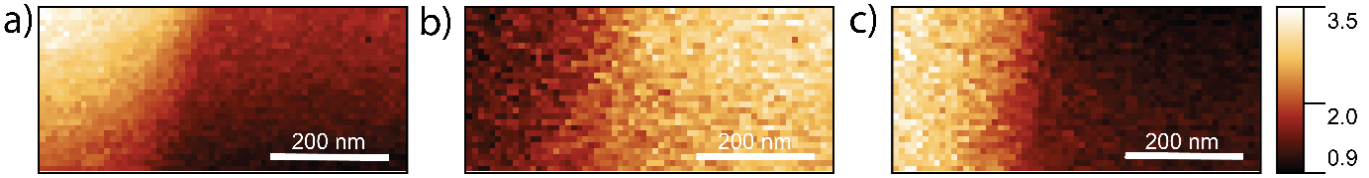

Figure 3. a), b), and c) TERS hyperspectral imaging of the square region (area of 640 nm x 320 nm) highlighted in image 1b, where the intensity renders the intensity of the 2D, G, and I_{2D}/I_G ratio.

To confirm the observed behaviour, we use a I_{2D}/I_G criteria (with confidence band) for all spectra measured; Figure 2g and Figure 2h illustrated these criteria for micro-Raman and TERS, respectively. Clearly, in the case of TERS measurements, we can clusterize the data into three categories: SLG with a $I_{2D}/I_G > 2.2$ (highlighted area in blue), BLG graphene with a $I_{2D}/I_G < 1.2$ (highlighted area in green), and a few data points that yield inconclusive results. This categorization allows for a clear distinction between SLG and BLG based on their respective I_{2D}/I_G criteria values with a resolution of around 60 nm. In contrast, for micro-Raman measurement, we observed the same categories, however, at the positions in the range between 93 nm and 700 nm, it falls into the inconclusive category. It is important to note that the I_{2D}/I_G criteria outlined in the ISO/TS 21356-1:2021 standard are specifically defined for green laser (λ = 532 nm) excitation and silicon subtraction. However, in this study, we employed a red excitation laser (λ = 632 nm) and a glass substrate. Although these variations were observed, they can potentially be applied in similar cases, showcasing the efficacy of TERS. This highlights the strength of TERS as a versatile technique.

The fact that TERS measurements were able to cluster a greater amount of data compared to micro-Raman measurements clearly confirms that TERS is a better technique for the task of labelling the number of graphene layers at the nanoscale. Moreover, we presented a complete hyperspectral map of an even smaller area. In the dashed area in Figure 1b, we performed a TERS experiment that presents enhancement factors of F_{2D}=4.1 and F_G=3.2 (measured by the ratio between the spectra acquired with PTTP and without PTTP) in SLG.

Within this specific region, TERS proved to be capable of distinguishing between SLG and BLG. Furthermore, by utilising the 2D and G peak heights (Figure 3a and Figure 3b) we generated images that revealed the presence of SLG, characterised by the more intense 2D peak area (and vice versa for G peak), and of BLG, represented by the less intense 2D peak area (and vice versa for G peak). Then, we used the I_{2D}/I_G criteria employed in each pixel to generate Figure 3c, further confirming these findings.

4. CONCLUSIONS

Experimental results obtained confirm the efficacy of TERS as a metrological tool for the characterization of SLG to BLG transitions at the nanoscale. Systematic TERS measurements, utilising the ISO/TS 21356-1:2021-1 standard's I_{2D}/I_G criteria, confirmed the capability of clusterizing SLG and BLG at the nanoscale. In contrast, the reliability of data clustering through Raman confocal measurements was found to be limited. The same measurement made by micro-Raman equipped with 1.4 N.A. objective generated an inconclusive region around 10x larger than when made by TERS.

TERS proved to be an extremely promising technique to be used as a metrological tool of practical and scientific interest for material characterisation. Therefore, it is strongly advisable to undertake further comprehensive research to encompass factors that can also change the I_{2D}/I_G ratio, which may disturb the shown criteria to distinguish SLG and BLG. For instance, the incident laser wavelength, substrate selection, method of graphene preparation, and, more importantly, the spectrometer intensity calibration prior to measurement can have an important effect on this ratio. It is important to note that the I_{2D}/I_G ratio is expected to be higher in TERS and dependent on the tip apex size and signal enhancement, as a consequence of Raman coherence, as reported by Cançado et al. [21]. Considering these aspects, there is significant potential for its inclusion as an alternative technique in forthcoming iterations of the ISO/TS 21356-1:2021 standard. By incorporating TERS into the standard, it would ensure that the latest advancements in material characterization are captured, and provide researchers and practitioners with a comprehensive framework for accurate and reliable measurements.

AUTHORS' CONTRIBUTION

Conceived and designed the analysis: Juan D. Caicedo, Tales F. S. Dias, Thiago L. Vasconcelos.

Collected the data: Juan D. Caicedo, Tales F. S. Dias.

Contributed data or analysis tools: Juan D. Caicedo, Braulio S. Archanjo, Thiago L. Vasconcelos.

Performed the analysis: Juan D. Caicedo, Tales F. S. Dias, Thiago L. Vasconcelos.

Wrote the paper: Juan D. Caicedo, Tales F. S. Dias, Thiago L. Vasconcelos.

ACKNOWLEDGEMENT

We acknowledge funding from the Coordenação de Aperfeiçoamento de Pessoal de Nível Superior (CAPES) and the Conselho Nacional de Desenvolvimento Científico e Tecnológico (CNPq).

REFERENCES

[1] Q. Ke, J. Wang, Graphene-based materials for supercapacitor electrodes – A review, Journal of Materiomics, 2, 1 (2016), pp. 37-54.
DOI: 10.1016/j.jmat.2016.01.001

[2] V. Berry, Impermeability of graphene and its applications, Carbon 62 (2013), pp. 1-10.
DOI: 10.1016/j.carbon.2013.05.052

[3] L. Zhao, R. He, K. T. Rim, T. Schiros, (+ 13 more authors), Visualizing Individual Nitrogen Dopants in Monolayer Graphene, Science, 333, 6045 (2011), pp. 999-1003.
DOI: 10.1126/science.1208759

[4] A. Zurutuza, C. Marinelli, Challenges and opportunities in graphene commercialization, Nature Nanotechnology, 9 (2014),

pp. 730-734.
DOI: 10.1038/nnano.2014.225

[5] J. Ribeiro-Soares, M. E. Oliveros, C. Garin, M. V. David, (+ 11 more authors), Structural analysis of polycrystalline graphene systems by Raman spectroscopy, Carbon, 95 (2015), pp. 646-652. DOI: 10.1016/j.carbon.2015.08.020

[6] C. Shen, C. Zhang, G. Cao, D. Liang, N. Liao, Waterproof strain sensor based on silver/graphene composite film for fine and large strain detection, Measurement, 239 (2025), 115482. DOI: 10.1016/j.measurement.2024.115482

[7] J. Wekalao, G. P. Srinivasan, S. K. Patel, F. A. Al-zahrani, Optimization of graphene-based biosensor design for haemoglobin detection using the gradient boosting algorithm for behaviour prediction, Measurement, 239 (2025), 115452. DOI: 10.1016/j.measurement.2024.115452

[8] J. M. de Oliveira Cremonezzi, H. Ribeiro, R. J. E. Andrade, G. J. M. Fechine, Characterization strategy for graphene oxide and molybdenum disulfide: Proceedings based on the ISO/TS 21356-1: 2021 standard, FlatChem 36 (2022), p. 100448. DOI: 10.1016/j.flatc.2022.100448

[9] D. Graf, F. Molitor, K. Ensslin, C. Stampfer, A. Jungen, C. Hierold, L. Wirtz, Raman mapping of a single-layer to double-layer graphene transition, The European Physical Journal Special Topics, 148 (2007), pp. 171-176. DOI: 10.1140/epjst/e2007-00237-1

[10] U. Schmidt, T. Dieing, W. Ibach, O. Hollricher, A confocal Raman-AFM study of graphene, Microscopy Today, 19, 6 (2011), pp. 30-33. DOI: 10.1017/S1551929511001192

[11] International Organization for Standardization. (2021). Nanotechnologies — Structural characterization of graphene (ISO/TS21356-1:2021). Online [Accessed 23 September 2025] https://www.iso.org/standard/70757.html

[12] C. Rabelo, H. Miranda, T. L. Vasconcelos, L. G. Cançado, A. Jorio, Tip-enhanced Raman Spectroscopy of Graphene, 4th International Symposium on Instrumentation Systems, Circuits and Transducers (INSCIT), Sao Paulo, Brazil, (2019), pp. 1-6. DOI: 10.1109/INSCIT.2019.8868627

[13] H. Miranda, C. Rabelo, T. L. Vasconcelos, L. G. Cançado, A. Jorio, Study of the interaction between light and nanoantennas in Tip-Enhanced Raman Spectroscopy, 4th International Symposium on Instrumentation Systems, Circuits and Transducers (INSCIT), Sao Paulo, Brazil, (2019), pp. 1-5. DOI: 10.1109/INSCIT.2019.8868513

[14] T. L. Vasconcelos, B. S. Archanjo, B. S. Oliveira (+ 6 more authors), Optical Nanoantennas for Tip-Enhanced Raman Spectroscopy, IEEE Journal of Selected Topics in Quantum Electronics, vol. 27, (2021), pp. 1-11. DOI: 10.1109/JSTQE.2020.3008526

[15] T. L. Vasconcelos, B. S. Archanjo, B. S. Oliveira, (+ 9 more authors), Plasmon-Tunable Tip Pyramids: Monopole Nanoantennas for Near-Field Scanning Optical Microscopy, Advanced Optical Materials, 6, 20 (2018), pp. 1-6. DOI: 10.1002/adom.201800528

[16] C. Rabelo, T. L. Vasconcelos, B. C. Publio, H. Miranda, L. G. Cançado, A. Jorio, Linkage between micro- and nano-raman spectroscopy of defects in graphene, Phys. Rev. Applied (2020), p. 024056. DOI: 10.1103/PhysRevApplied.14.024056

[17] B. S. Oliveira, B. S. Archanjo, R. Valaski, C. A. Achete, L. G. Cançado, A. Jorio, T. L. Vasconcelos, Nanofabrication of plasmon-tunable nanoantennas for tip-enhanced Raman spectroscopy, The Journal of Chemical Physics, 14 (2020), 024056. DOI: 10.1063/5.0021560

[18] M. D. Sonntag, E. A. Pozzi, N. Jiang, M. C. Hersam, R. P. Van Duyne, Recent advances in tip-enhanced Raman spectroscopy, The Journal of Physical Chemistry Letters, 16 (2014), pp. 5555-5571. DOI: 10.1021/jz5015746

[19] Z. F. Cai, N. Kumar, R. Zenobi, Probing On-Surface Chemistry at the Nanoscale Using Tip-Enhanced Raman Spectroscopy, CCS Chemistry, 5 (2023), pp. 55-71. DOI: 10.31635/ccschem.022.202202287

[20] M. Huang, P. V. Bakharev, Z. J. Wang, (+ 14 more authors), Large-area single-crystal AB-bilayer and ABA-trilayer graphene grown on a Cu/Ni(111) foil, Nature Nanotechnology, 15 (2020), pp. 289-295. DOI: 10.1038/s41565-019-0622-8

[21] L. G. Cançado, R. Beams, A. Jorio, L. Novotny, Theory of Spatial Coherence in Near-Field Raman Scattering, Phys. Rev. X, 4 (2014), 031054. DOI: 10.1103/PhysRevX.4.031054